Molecular Therapy
Original Article

Dose-Dependent Prevention of Metabolic and Neurologic Disease in Murine MPS II by ZFN-Mediated *In Vivo* Genome Editing

Kanut Laoharawee,[1,4] Russell C. DeKelver,[2,4] Kelly M. Podetz-Pedersen,[1] Michelle Rohde,[2] Scott Sproul,[2] Hoang-Oanh Nguyen,[2] Tam Nguyen,[1] Susan J. St. Martin,[2] Li Ou,[3] Susan Tom,[2] Robert Radeke,[2] Kathleen E. Meyer,[2] Michael C. Holmes,[2] Chester B. Whitley,[3] Thomas Wechsler,[2] and R. Scott McIvor[1]

[1]Center for Genome Engineering, Department of Genetics Cell Biology and Development, University of Minnesota, Minneapolis, MN, USA; [2]Sangamo Therapeutics, Inc., 501 Canal Boulevard, Richmond, CA, USA; [3]Gene Therapy Center, Department of Pediatrics, University of Minnesota, Minneapolis, MN, USA

Mucopolysaccharidosis type II (MPS II) is an X-linked recessive lysosomal disorder caused by deficiency of iduronate 2-sulfatase (IDS), leading to accumulation of glycosaminoglycans (GAGs) in tissues of affected individuals, progressive disease, and shortened lifespan. Currently available enzyme replacement therapy (ERT) requires lifelong infusions and does not provide neurologic benefit. We utilized a zinc finger nuclease (ZFN)-targeting system to mediate genome editing for insertion of the human IDS (hIDS) coding sequence into a "safe harbor" site, intron 1 of the albumin locus in hepatocytes of an MPS II mouse model. Three dose levels of recombinant AAV2/8 vectors encoding a pair of ZFNs and a h*IDS* cDNA donor were administered systemically in MPS II mice. Supraphysiological, vector dose-dependent levels of IDS enzyme were observed in the circulation and peripheral organs of ZFN+donor-treated mice. GAG contents were markedly reduced in tissues from all ZFN+donor-treated groups. Surprisingly, we also demonstrate that ZFN-mediated genome editing prevented the development of neurocognitive deficit in young MPS II mice (6–9 weeks old) treated at high vector dose levels. We conclude that this ZFN-based platform for expression of therapeutic proteins from the albumin locus is a promising approach for treatment of MPS II and other lysosomal diseases.

INTRODUCTION

Mucopolysaccharidosis type II (MPS II) (Hunter syndrome) is a rare, X-linked recessive inherited disorder caused by deficiency of the lysosomal hydrolase iduronate 2-sulfatase (IDS). IDS catalyzes the first step in the metabolic pathway for lysosomal degradation of glycosaminoglycans (GAGs) heparan and dermatan sulfate. IDS deficiency results in lysosomal GAG accumulation, leading to skeletal dysplasia, cardiac and respiratory obstruction, organomegaly, and, in severe cases, neurologic impairment and death by 10 years of age. Enzyme replacement therapy (ERT) is the only available US Food and Drug Administration (FDA)-approved treatment for MPS II. ERT is used to manage but not eliminate disease progression, requires frequent enzyme infusions for the lifetime of the patient, and does not prevent the emergence of neurologic disease. New therapeutic approaches are thus greatly needed to address limitations in the currently available treatment.

Adeno-associated virus (AAV) vectors have shown great promise for therapeutic gene transfer and correction of monogenic disease.[1,2] The standard approach for AAV gene transfer to the liver has been to deliver a cDNA expression cassette as an extrachromosomal episome.[3] However, a major drawback for this platform is dilution of the transgene episome in a setting of substantial cell proliferation, such as the growing liver in a pediatric patient population.[3]

The emergence of genome editing has provided the means to achieve sustained therapeutic gene expression in a variety of pre-clinical models.[3–6] Compared to non-specific integration approaches, genome editing systems, such as zinc finger nucleases (ZFNs), allow transgene insertion at a specific targeted position, which minimizes the risk of non-specifically altering expression of nearby oncogenes. The general approach of site-specific gene editing is to target the disease locus itself; however, the level of expression from the disease locus may not be sufficient to render a therapeutic effect. Targeted insertion of a therapeutic transgene into a well-characterized, highly transcriptionally active locus ("safe harbor") addresses this issue. In contrast to episomal cDNA vectors, site-specific gene insertion by ZFNs ensures that the therapeutic gene will be replicated during cell proliferation and allows for undiluted, sustained expression of the therapeutic protein.

We have developed an AAV-based *in vivo* genome editing approach using ZFNs to mediate targeted insertion of therapeutic sequences into the albumin locus in hepatocytes.[3] The albumin locus was selected as a genomic safe harbor because albumin is expressed at a very high level in the liver, leading to high levels

Received 24 October 2017; accepted 31 January 2018;
https://doi.org/10.1016/j.ymthe.2018.03.002.

[4]These authors contributed equally to this work.

Correspondence: R. Scott McIvor, PhD, Department of Genetics Cell Biology and Development, University of Minnesota, Minneapolis, MN, USA.
E-mail: mcivo001@umn.edu

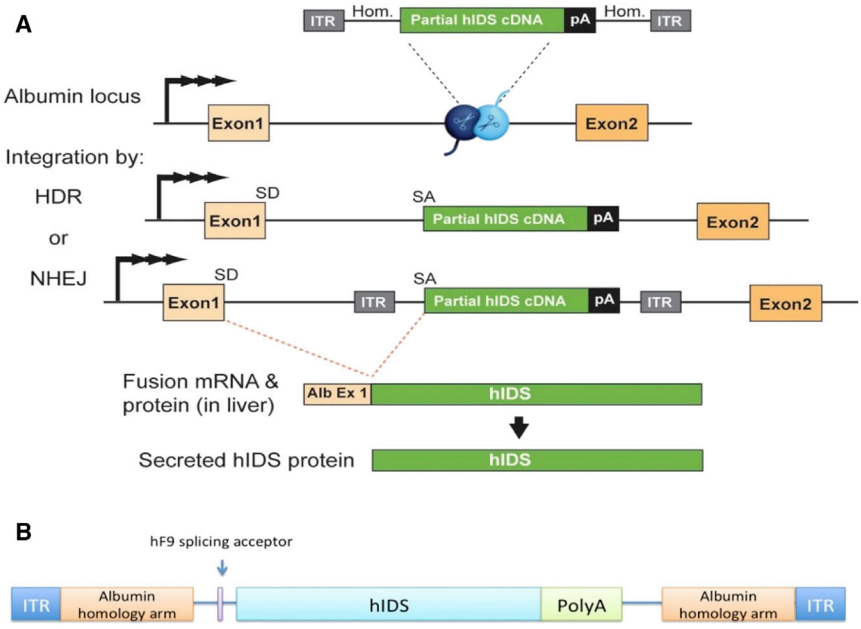

Figure 1. Schematic Showing ZFN-Mediated h*IDS* Gene Transfer and Expression from the Albumin Locus

(A) Outline of strategy for ZFN-mediated integration of h*IDS* at intron 1 of the albumin locus in mouse hepatocytes. (B) Expression cassette of promoterless h*IDS* cDNA donor construct is shown. A hF9 splice acceptor is followed by the h*IDS* cDNA sequence and rabbit globin polyadenylation signal flanked on both 5′ and 3′ ends with mouse albumin homology arms and AAV2 ITR sequences.

of circulating albumin. In this strategy, the desired transgene, beginning with a splice acceptor signal, is inserted into intron 1 of the albumin locus. The resultant mRNA transcript includes sequences from exon 1 of the albumin locus encoding a secretory peptide that is cleaved from the final protein product with subsequent secretion of the desired transgene product into the circulation (Figure 1). Using this strategy, the albumin locus has been successfully edited using ZFNs for insertion of human coagulation factor VIII (hF8) and factor IX (hF9) transgenes and subsequent correction of clotting defects in mouse models of hemophilia A and B, respectively.[3,4,7] Here, we report extension of this platform to include effective AAV2/8-mediated expression of albumin-specific ZFNs for inserting the human IDS (h*IDS*) coding sequence into intron 1 of the albumin locus, resulting in long-term expression of hIDS protein and correction of IDS deficiency in an MPS II mouse model. These results demonstrate the effectiveness of this approach and its potential as a therapeutic strategy for treatment of the mucopolysaccharidoses, clinical testing of which for MPS II was initiated in November 2017 (ClinicalTrials.gov identifier: NCT03041324) for the first ever evaluation of *in vivo* genome editing in humans.

RESULTS

Dose-Dependent ZFN Activity at Intron 1 of Albumin Locus

To determine the effectiveness of *in vivo* site-specific h*IDS* sequence insertion into intron 1 of the albumin locus, male MPS II mice between 6 and 9 weeks of age were injected with one of three increasing dose levels of three AAV2/8 vectors encoding a pair of ZFNs targeting intron 1 of the albumin locus along with a h*IDS* donor (Table 1; Figure 1). Vectors were administered as a single tail-vein injection at a ZFN:ZFN:donor ratio of 1:1:8. Another group of MPS II mice was injected with AAV2/8 donor only (i.e., omitting ZFN-expressing vectors). Unaffected MPS II and wild-type littermates were injected with formulation buffer as control groups. MPS II ($IDS^{y/-}$) mice show no detectable plasma or tissue IDS activity and have been shown to exhibit phenotypic features typical for MPS II, such as skeletal and craniofacial abnormalities, hepatosplenomegaly, neurological deficits, shortened lifespan, and increased GAG levels in tissues and urine.[8–11] This study was based on a disease prevention paradigm, where mice in an early stage of disease development were administered ZFNs and donor and followed over 4 months.

ZFN activity in targeted hepatocytes was measured by deep sequencing at intron 1 of the mouse albumin locus using the MiSeq system (Illumina). Analysis of the liver showed that the percent insertions and deletions (% indels) of ZFN+donor-treated groups increased in a dose-dependent manner at both 1 month (mean values of 12.6%, 31.7%, and 49.3% for low, mid, and high doses, respectively) and 4 months (mean values of 26.4%, 43.5%, and 56.0% for low, mid, and high doses; Figure 2A) post-treatment. There was no gene modification observed in the donor only group or in either of the formulation control groups. These results demonstrate that ZFNs were highly active in modifying intron 1 of the mouse albumin locus in hepatocytes *in vivo*.

Following confirmation of ZFN activity, site-specific insertion of the h*IDS* transgene was assessed using a radiolabeled PCR assay that distinguishes between insertion via non-homologous end joining (NHEJ) and homology-directed repair (HDR) pathways. The results indicate that, at 1 month and 4 months after treatment, targeted insertion of the h*IDS* transgene occurred in hepatocytes of ZFN+donor-treated mice and that the insertion occurred by both NHEJ and HDR (Figure S1). The high-dose ZFN+donor animals showed a more intense signal for both the HDR and NHEJ PCR product bands, indicating higher rates of h*IDS* insertion, consistent with higher ZFN activity (% indels) in this group. These data indicate that ZFN activity determined by % indels at the albumin locus is predictive of the efficiency of targeted h*IDS* donor insertion.

Table 1. Group Designations and Dose

Group	Group Designation	Genotype	No. of Animals	Each ZFN Dose Level (vg/Mouse)	Donor Dose Level (vg/Mouse)	Total AAV Dose (vg/Mouse)
1	formulation buffer control	C57BL/6 wild-type littermates	13	0	0	0
2	formulation buffer control	MPS II littermates	13	0	0	0
3	ZFNs+donor low dose	MPS II	8	2.50E+10	2.00E+11	2.50E+11
4	ZFNs+donor mid dose	MPS II	8	5.00E+10	4.00E+11	5.00E+11
5	ZFNs+donor high dose	MPS II	13	1.50E+11	1.20E+12	1.50E+12
6	donor only	MPS II	8	0	4.00E+11	4.00E+11

Supraphysiological, Vector Dose-Dependent IDS Activity Levels in the Liver

Western blot analysis further confirmed the presence of hIDS in the livers of ZFN+donor mice at 1 and 4 months post-injection (Figure 2B). hIDS protein in ZFN+donor mice was expressed in a dose-dependent manner at both time points. Two of the animals shown in Figure 2B (1323 and 1264) showed neither evidence of vector genomes nor ZFN activity, so these were likely failed injections and were therefore omitted from Figure 2A. One mouse (1320) showed a low signal on western blot but detectable ZFN activity and IDS enzyme activity in plasma and tissues (see below). No hIDS-specific bands were detected in formulation-treated MPS II or donor-only-treated mice at either time point. Detection of hIDS protein thus required the presence of both ZFNs and the h*IDS* donor.

All ZFN+donor groups exhibited dose-dependent IDS activity levels in the liver at 1 month (mean values of 265, 1,756, and 2,479 nmol/hr/mg for the low-, mid-, and high-dose groups, respectively; Figure 3A) and 4 months (519, 1,696, and 5,355 nmol/hr/mg protein for the low-, mid-, and high-dose groups, respectively; Figure 3B) post-treatment. The levels of IDS activity in all three ZFN+donor groups were significantly higher than control MPS II mice and were 20-, 66-, and 207-fold higher than levels found in wild-type mice at 4 months (Figure 3B).

Supraphysiologic Levels of Circulating IDS Enzyme following ZFN-Mediated hIDS Gene Transfer into MPS II Mice

Blood was collected at different time points post-injection throughout the study to evaluate plasma IDS enzyme activity. No plasma IDS activity was detected in untreated MPS II mice (Figure 4). Low levels of plasma IDS activity (less than 0.6 nmol/hr/mL) were observed in wild-type mice and in MPS II mice that received donor only. By contrast, we observed a clear, dose-dependent increase in levels of plasma IDS activity in ZFN+donor-treated MPS II mice. From day 14, the levels of plasma IDS were significantly increased in the mid- and high-dose groups (mean of 18 and 60.9 nmol/hr/mL, respectively) when compared to the level of activity in the control groups. The level of IDS in plasma persisted through 120 days in mice that received ZFN+donor at low, mid, and high dose (mean values of 6.5, 23.7, and 63.2 nmol/hr/mL, respectively). Plasma IDS activity levels were increased an average of 20-, 80-, and 200-fold higher than wild-type C57BL/6 littermates. These results demonstrate that stable supraphysiological levels of circulating IDS were achieved after a single intravenous (i.v.) injection of AAV2/8 vectors encoding mouse surrogate ZFN and a homologous h*IDS* donor targeting intron 1 of the albumin locus in MPS II mice. Notably, the sustained levels of hIDS activities in all ZFN+donor mice indicate that hIDS may not be immunogenic in C57BL/6 mice.

Circulating hIDS Leads to Cross-Correction of IDS Deficiency in Tissues of MPS II Mice

Following confirmation of hIDS secretion into the circulation, we next examined secondary tissues for enzyme uptake and potential cross-correction in these tissues. The promoters regulating both ZFN expression (the human α-1-antitrypsin [hAAT] promoter in combination with the apolipoprotein E [ApoE] enhancer) and endogenous albumin expression are liver specific. Therefore, neither ZFN activity nor h*IDS* insertion is expected in non-hepatic tissues, and even in the event of h*IDS* gene insertion at the albumin locus in one of these tissues, hIDS would not be expressed. As such, any increase in IDS activity observed in tissues outside of the liver must result from enzyme uptake following secretion from the liver into the bloodstream. The liver specificity of the ApoE/hAAT enhancer and promoter was confirmed in a separate study in wild-type mice, in which no ZFN activity was observed in tissues other than liver (Figure S2).

In the present study in MPS II mice, observed levels of IDS activity in the heart, spleen, kidney, and muscle tissues at day 28 and day 120 in all 3 ZFN+donor groups were similar to or higher than wild-type levels, and significant activity was also observed in the lung (Figures 3A and 3B). IDS activity in the donor only group was undetectable or markedly lower (~160- to 250-fold lower) than that observed in the ZFN+donor groups. Notably, we observed 1.5% of wild-type IDS activity in the brain of high-dose ZFN+donor-treated mice (mean values of 4.61 versus 305.23 nmol/hr/mg in high-dose and wild-type control groups, respectively). Overall, these results suggest that a high level of IDS was expressed in the liver and released into the circulation, from which other secondary organs efficiently took up the circulating enzyme.

IDS cellular uptake and subsequent lysosomal targeting is dependent upon the mannose-6-phosphate (M6P) receptor.[12] To confirm that

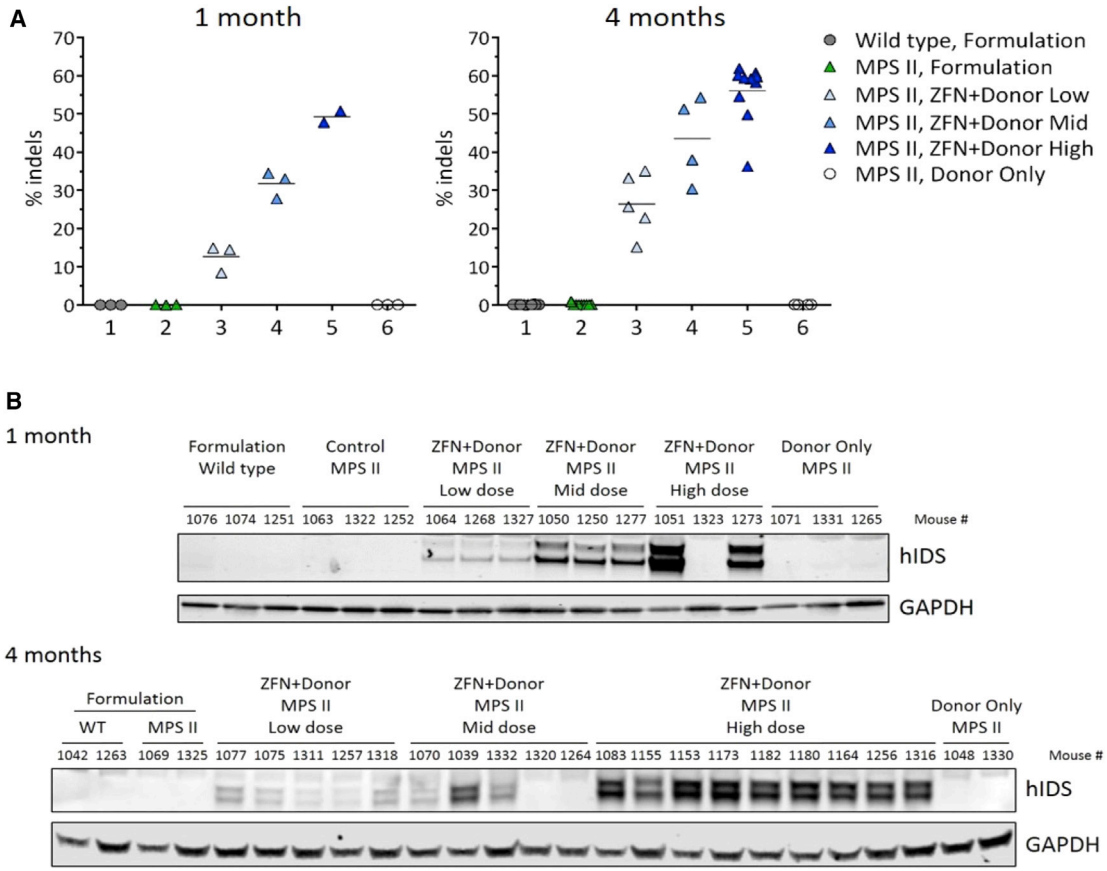

Figure 2. Albumin Gene Modification and Expression of hIDS in Mouse Hepatocytes

(A) Percent indels were determined in DNA extracted from the livers of animals indicated in the key to the right as described in Materials and Methods. Horizontal line represents mean % indels within each group. Dose-dependent ZFN activity was detected in all groups of mice 1 and 4 months after receiving ZFN+donor. Two animals (no. 1264 and no. 1323) showed no ZFN activity, indicating a failure of the injection (see text). Data from animal numbers 1264 and 1323 were thus excluded from all statistical analyses. No ZFN activity was detected in donor only, wild-type, and MPS II control animals. (B) Western blot of hIDS using a human-specific IDS antibody showed consistent levels of hIDS protein correlated to ZFNs % indel activities.

hIDS produced from the albumin locus is appropriately modified by mannose-6-phosphorylation, we performed cellular uptake experiments *in vitro* using human albumin ZFNs in the human hepatoma cell line HepG2 to demonstrate that excess M6P can inhibit albumin-produced hIDS from entering secondary cells (Figure S3). Taken together, these *in vivo* and *in vitro* results demonstrate that hIDS produced from the albumin locus is efficiently taken up by secondary tissues for cross-correction in an M6P-dependent manner.

Marked Reduction of Tissue and Urine GAGs in All ZFN+Donor-Treated Groups

At the end of the study, tissues were collected and processed to measure GAG storage, the natural IDS substrate and a biomarker of MPS II disease. As anticipated, GAG contents in all of the tested tissues of formulation buffer-treated MPS II mice were markedly increased compared to wild-type mice (Figures 5A and 5B). In contrast, all ZFN+donor-treated groups showed GAG reduction at 1 month post-treatment (Figure 5A). At 4 months (Figure 5B), high-dose ZFN+donor-treated mice showed normalization of GAG levels in all tissues evaluated except brain. Mid- and low-dose ZFN+donor-treated mice further showed significant reduction of tissue GAG levels when compared to MPS II controls. In contrast, donor-only-treated mice showed GAG contents relatively comparable to MPS II control mice. Notably, observed GAG levels in wild-type mice were higher in the brain than in other tissues. This finding may be due to the assay used, as it detects total sulfated GAGs and the brain is known to have high levels of chondroitin sulfate.[13] An enrichment of chondroitin sulfate relative to other tissues could potentially mask any decreases in dermatan and heparan sulfate in the brain. As such, brain homogenates were further analyzed for dermatan and heparan sulfate levels by mass spectrometry. Results demonstrated a trend toward reduction of dermatan sulfate levels with increasing ZFN+donor dose, reaching significance in the high-dose group (Figure 5C). However, there was also a trend toward lower dermatan sulfate levels in the group treated with donor alone, and a trend but no significant effect was observed on heparan sulfate levels.

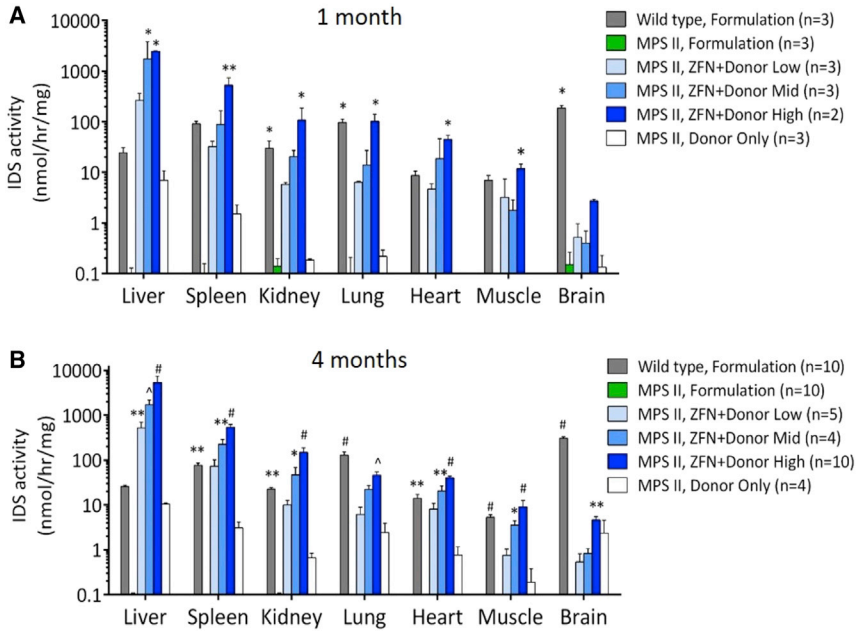

Figure 3. Tissue IDS Activities at 1 Month and 4 Months Post-treatment

(A) IDS activities in tissue extracts were determined as described in Materials and Methods. IDS activities increased in a dose-dependent fashion in the ZFN+donor-treated groups at 1 month. (B) At 4 months, IDS activities in all ZFN+donor-treated groups were significantly higher than the MPS II formulation control group and were expressed in a dose-dependent manner. We observed significantly higher IDS activities than wild-type in the liver of all ZFN+donor-treated groups. IDS activities were higher or comparable to wild-type levels in other tissues except brain. IDS activity was not detected in any formulation-treated MPS II tissue. Brain IDS activities in the high-dose group were 1.5% of the wild-type level. Data shown are means ± SEM. *$p < 0.05$; **$p < 0.01$; ^$p < 0.001$; #$p < 0.0001$ versus the formulation-treated MPS II control group.

The accumulation of GAGs in tissues leads to characteristic lysosomal vacuolation that can be observed microscopically. As part of our histopathologic assessment, the amount of vacuolation was evaluated from a subset of tissues (brain, heart, lung, liver, skeletal muscle, and spleen) collected at the 1-month necropsy and a full set of tissues (see Table S1) collected at the 4-month necropsy. MPS-II-related vacuolation was evident in the brain, heart (valve and vascular), liver, lung, and other tissues, and these changes were consistent with IDS deficiency in the MPS II mouse model. At the 1-month interim necropsy in ZFN+donor-treated mice, variably decreased vacuolation was observed in the lung, heart valves, large elastic arteries of the heart, spleen, and liver and was attributed to ZFN+donor treatment, although reduced vacuolation was not observed in the brain. When compared with the interim 1-month necropsy, control MPS II animals necropsied at 4 months had an increased incidence and/or severity of typical vacuolation of various cell types in the tissues examined that were consistent with lysosomal accumulation of GAGs. In contrast, ZFN+donor-treated mice displayed partial or complete correction of cellular vacuolation in a wide array of tissues, including the sciatic nerve, lung, and heart valve (Figure 5D; Table S1). In addition, administration of ZFN+donor or donor only to MPS II mice was well tolerated, and there were no test article-related toxicological findings in treated animals. The ZFN+donor-mediated clearance of lysosomal storage material did not result in any unintended microscopic findings or toxicity.

Urine was collected prior to injection and on days 7, 14, 21, 28, 42, 60, 74, 90, 105, and 120 to determine whether restoration of IDS in the ZFN+donor-treated mice affected urinary GAG excretion. The MPS II control group (formulation-treated) showed an elevation of GAG content in the urine that was maintained throughout the experiment. In contrast, we observed a reduction in urine GAG content to levels observed in wild-type mice by day 14 in the mid- and high-dose treatment groups (Figure S4) and by day 21 in the low-dose group. Reduced urine GAG levels were maintained throughout the study (day 120) and were similar to the wild-type level.

Combined, these results show that both ZFNs and the h*IDS* donor are required to produce sustained supraphysiological IDS in the circulation with subsequent significant reduction of GAG storage in tissues.

Sustained High-Level IDS Expression Prevents Neurocognitive Deficiency in MPS II Mice

At 4 months post-treatment, all mice were tested in the Barnes maze to evaluate neurocognitive function as described in Materials and Methods. In this test, it is anticipated that a cognitively normal mouse will display a progressive reduction in the amount of time required to escape the platform over successive days of testing. As shown in Figure 6A, there was a reduction in the average time required for wild-type mice to escape the platform between day 1 (160 s) and day 6 (23 s), as expected. There was also a reduction in the time to escape (from 160 s down to 67 s) for formulation-treated MPS II mice during the first 3 days of training, but there was no further improvement in performance observed for these mice on days 4–6. MPS II mice thus exhibit a neurocognitive deficit in this test. Interestingly, the time required for animals in the high-dose ZFN+donor group to escape the platform was similar to that of the wild-type animals, decreasing from 140 s to 31 s over 6 days of training. The time required to escape the platform was significantly different on days 4 and 6 between formulation-treated MPS II and high-dose ZFN+donor mice ($p < 0.05$). This effect is more clearly observed when results from individual mice on day 6 of testing are examined, in which 9/10 high-dose ZFN+donor mice performed indistinguishably from wild-type (Figure 6B). In contrast, the time required to escape the

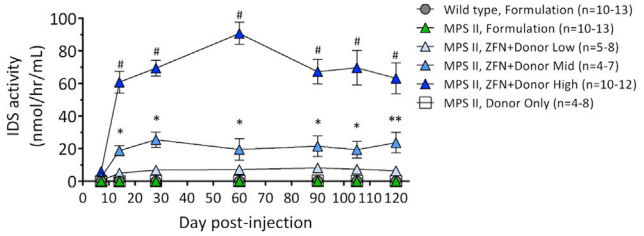

Figure 4. Plasma IDS Activity after Administration of AAV2/8 Delivering ZFNs and h*IDS* Donor

Three different doses of ZFN+donor were injected into each of three different groups of MPS II mice. One group of mice received only h*IDS* donor (donor only). Wild-type littermates and MPS II littermates were injected with formulation buffer. Plasma was periodically collected post-treatment until day 120 post-injection. Data shown are means ± SEM. *p < 0.05; **p < 0.01; #p < 0.0001 versus wild-type group.

platform among formulation-treated MPS II mice, low-dose and mid-dose ZFN+donor group, as well as donor only group was not significantly different (data not shown). ZFN-mediated h*IDS* sequence insertion at albumin locus in the liver thus resulted in sustained, high-level IDS activity in the circulation that prevented neurocognitive impairment in a murine model of MPS II.

DISCUSSION

In this paper, we describe use of our previously reported ZFN targeting system for *in vivo* site-specific insertion of the h*IDS* coding sequence into intron 1 of the albumin locus in hepatocytes of MPS II mice, thereby achieving high-level expression of hIDS in the liver and secretion of hIDS into the circulation at up to 200 times the wild-type level of plasma IDS. The levels of hIDS achieved in the circulation increased in a dose-dependent manner, and IDS was subsequently taken up from the circulation by secondary tissues, resulting in normalization of GAG storage levels. Remarkably, the high level of IDS expression achieved in animals administered the highest dose of ZFN+h*IDS* donor encoding vectors prevented emergence of a neurocognitive deficit exhibited in control MPS II animals.

AAV vector-mediated gene transfer has been extensively evaluated in many pre-clinical and clinical studies, highlighting its potential for gene therapy.[2,14,15] However, episomal expression of a transgene in the liver is unlikely to achieve long-term expression in a pediatric patient population, due to the high proliferative rate of hepatocytes in this population.[16] By contrast, targeted transgene insertion can be used to avoid dilution of therapeutic transgene in the liver, and previous studies have shown that transgene insertion into the genome can be applied successfully to achieve therapeutic benefit.[3,4,7] The albumin locus was used for targeted insertion of the IDS sequence in this study because of its tractability and because of its very high level of expression in the liver.[3] The effectiveness of this strategy has been previously demonstrated in murine models of hemophilia A and hemophilia B.[1,3,7] Here, we demonstrate that targeted insertion of a promoterless h*IDS* cDNA at intron 1 of the albumin locus in hepatocytes is an efficient system to achieve therapeutic outcomes for MPS II in a murine model.

A previous study reported that AAV-mediated targeting of the albumin locus with a promoterless vector donor alone may achieve transgene insertion sufficient to correct disease.[17] In our study, we observed levels of IDS activity in the circulation of animals treated with the donor only vector, i.e., omitting ZFN-expressing vectors, of ~100-fold lower than those achieved in the high-dose ZFN+donor mice, and we found that this was insufficient for correction of disease phenotypes. Neither GAG correction in tissues nor prevention of neurologic deficit was observed in the donor only group. In contrast, all mice that received ZFN+donor exhibited dose-dependent supraphysiological IDS activity in the circulation with significant GAG reduction in tissues. We thus found that ZFN-mediated introduction of double-strand breaks was necessary to achieve sufficient insertion into the albumin locus for high-level expression and circulation of hIDS with subsequent metabolic correction and neurologic benefit in the murine model of MPS II.

ZFN+donor-treated MPS II mice showed striking results for sustained supraphysiological levels of IDS activity in the circulation that persisted for at least 4 months post-treatment. Circulating enzyme in the three ZFN+donor-treated groups (low, mid, and high doses) thus provided substantial amounts of enzyme for metabolic cross-correction and normalization of GAG content in secondary organs. Microscopic evaluation of tissues at 1 and 4 months further demonstrated reduced lysosomal vacuolation following ZFN+donor administration. Interestingly, sustained high levels of enzyme also resulted in improved neurocognitive outcome as demonstrated in the Barnes maze for the high-dose ZFN+donor group. These results imply that a fraction of IDS protein penetrated the blood brain barrier, thereby gaining access to the CNS. This phenomenon is consistent with previous studies in which high levels of ERT were administered over a sufficient period of time.[18–22] The constant high level of enzyme in the circulation in the current approach likely contributes to effectiveness in penetrating the CNS. Approximately 1.5% of the wild-type level of IDS activity in the brain was observed (approximately 5 nmol/hr/mg protein) in the high-dose group. This level of IDS enzyme correlated with a benefit in neurocognitive performance. This novel discovery suggests that IDS activity in the brain of 1.5% of wild-type is sufficient to prevent neurologic deficit in MPS II mice when treatment is administered at a young age (6–9 weeks old). Although we have detected enzyme activity in brain extracts from treated animals, this could be the result of enzyme taken up by the microvascular endothelial cells in the brain, despite the perfusion performed on these animals prior to euthanization. Further investigation is needed to address this issue as well as the mechanism of neurocognitive improvement in the MPS II mouse model without reduction of GAGs in the brain to wild-type levels. Regardless of improvement in neurologic outcome, a non-invasive one-time procedure that results in sustained and high levels of therapeutic enzyme demonstrates the promise of this approach for the treatment of

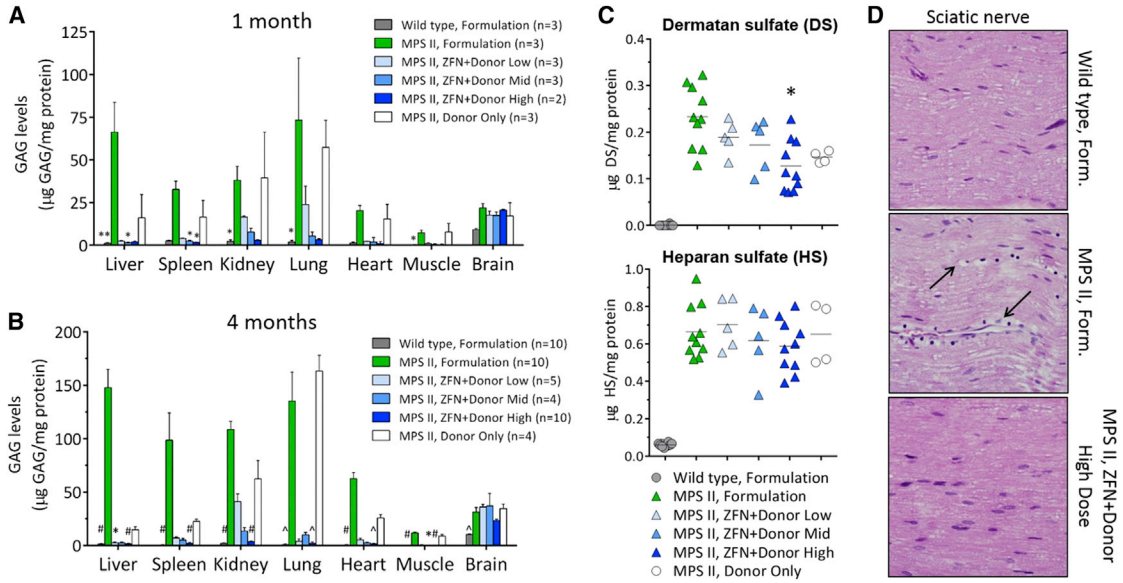

Figure 5. Glycosaminoglycan Content in Tissues Post-injection

Levels of tissue GAGs at 1 month (A) and 4 months (B) in MPS II control animals were significantly elevated when compared to wild-type. GAG contents were reduced or normalized in all tissues tested (except brain) in all treated groups at 1 and 4 months post-treatment. *$p < 0.05$; **$p < 0.01$; ^$p < 0.001$; #$p < 0.0001$ versus the formulation-treated MPS II control group. (C) Levels of dermatan and heparan sulfate in mouse brain homogenates, 4 months post-injection, are shown. Horizontal lines represent the mean of each group. All wild-type mice had levels of dermatan sulfate at or below the lower limit of quantification for this assay (< 0.005 µg DS/mg protein lysate); *$p < 0.05$ for high-dose-treated versus untreated MPS II mice. Data shown are means ± SEM. (D) Correction of cellular vacuolation in ZFN+donor-treated MPS II mice is shown. Tissue sections collected from all animals were fixed in 10% neutral-buffered formalin, embedded in paraffin, and processed to slides. Slides were stained with H&E and evaluated by a board-certified veterinary pathologist (Seventh Wave Laboratories) for potential evidence of pathology and degree of tissue vacuolation. Images are shown at 40× magnification. Arrows indicate the location of disease-related microvesiculated mesenchymal cells. A complete list of corrected tissues is in Table S1.

MPS II and the improvement of patient quality of life through the reduction or elimination of the need for lifelong ERT.

In conclusion, our results demonstrate that systemic administration of AAV2/8 vectors encoding a pair of ZFNs and the h*IDS*-donor-targeting insertion into the intron 1 of the mouse albumin locus results in high-level expression of hIDS activity in the liver with subsequent secretion into the bloodstream and widespread IDS enzyme distribution. Supraphysiological levels of IDS activity not only leads to cross-correction of the enzyme deficiency in other tissues but also to metabolic correction of GAG storage. For the first time, we present here that high ZFN-mediated IDS expression had a profound effect on preventing neurocognitive impairment in a mouse model of MPS II when treated at young age. These results constitute definitive proof of concept for clinical application of AAV-mediated *in vivo* targeting of the albumin locus for human MPS II, for which we envision that consistent, high-level expression of hIDS with secretion into the circulation and systemic distribution will provide improved therapy over currently available treatments. Our observations suggest that albumin-specific genome editing is a promising approach for the treatment of the mucopolysaccharidoses as well as other lysosomal disorders. For MPS II, Sangamo Therapeutics has developed a ZFN pair and an IDS donor construct targeting intron 1 of the human albumin locus packaged using AAV6 capsid. Based on the results described here and additional pre-clinical data, a phase 1 clinical study has been approved by the FDA (ClinicalTrials.gov identifier: NCT03041324), and the first patient was recently infused, the first human application of *in vivo* genome editing.

MATERIALS AND METHODS

Study Design

All animal care and experimental procedures were evaluated and approved by the Institutional Animal Care and Use Committee of the University of Minnesota. C57BL/6 mice deficient in IDS were kindly provided by Dr. Joseph Muenzer (University of North Carolina, NC, USA). Animals were maintained under specific pathogen-free conditions at Research Animal Resources (RAR) of the University of Minnesota. Male pups were generated from IDS heterozygous females (IDS $^{+/-}$) mated with C57BL/6 males (IDS $^{y/+}$).

The vectors were prepared by Sangamo Therapeutics and were stored as received at −70°C until use. Three engineered AAV2/8 vectors were used in this study; two AAV vectors encode the two ZFNs (ZFNs) and one AAV vector encodes the promoterless h*IDS* transgene DNA template (donor) flanked by mouse albumin intron 1 homology arms.

The AAV2/8 vectors were diluted into formulation buffer (PBS supplemented with 35 mM NaCl and 5% glycerol [pH 7.1]) to the doses shown

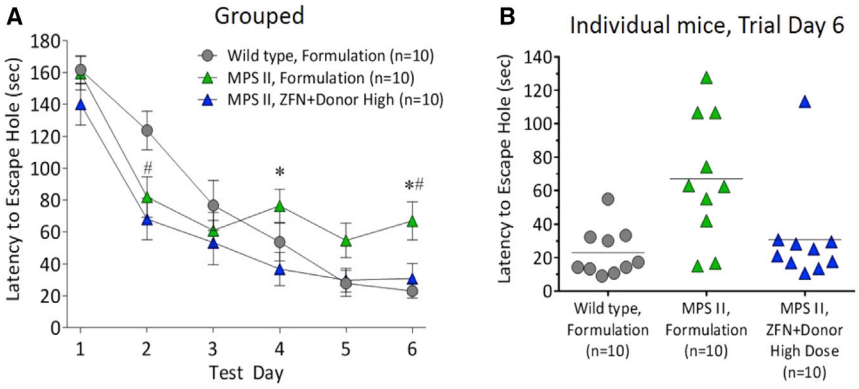

Figure 6. Barnes Maze Performance of High-Dose ZFN+Donor-Treated Group at 4 Months Post-injection

Cognitive performance was assessed using the Barnes maze at 4 months post-treatment. (A) Data represent mean ± SEM of the time required to escape the platform over 6 days of testing. Wild-type and high-dose ZFN+donor groups showed significantly better performance when compared to MPS II control animals ($p < 0.05$; *MPS II formulation versus ZFN+donor high; #MPS II formulation versus wild-type). Performance comparable to wild-type was observed in the high-dose group. Mid-dose, low-dose, and donor-only groups did not perform better than the formulation-treated MPS II control group (data not shown). (B) Data from individual mice on day 6 of testing are shown. Data shown are means ± SEM.

in Table 1. MPS II mice between 6 and 9 weeks of age were randomly assigned to groups 2–6, and unaffected C57BL/6 littermates were assigned to group 1. The mice in groups 1 and 2 were injected i.v. with vehicle, i.e., formulation buffer, and MPS II mice in groups 3–6 were injected i.v. with a combination of vectors at different doses as shown in Table 1. The total dose volume injection was 200 μL per mouse.

AAV Vector Constructs and Packaging

The heterodimeric ZFNs targeting intron 1 of the mouse albumin locus containing the obligate heterodimer ELD/KKR mutations in the FokI domain[23] (ZFNs 48641 and 31523) and the h*IDS* donor construct have been previously described.[3] The h*IDS* donor construct contains a codon-optimized hIDS cDNA lacking the endogenous IDS signal peptide, a hF9 splice acceptor sequence, and arms of homology to the mouse albumin target site of approximately 600 bp in length in total (Figure 1B). Recombinant AAV2/8 vectors (comprised of AAV2 ITRs and the AAV8 capsid) were produced by triple transfection of 293 cells in 10-chamber CELLSTACK culture chambers (Corning), purified by cesium chloride density gradient centrifugation followed by dialysis, and titered as previously described.[3]

Blood, Urine, and Tissue Collection

Approximately 200 μL of blood was collected via submandibular puncture from all animals to assess IDS activity on days 7, 14, 28, 60, 90, and 105 and at necropsy (approximate day 120). Blood was collected into heparinized tubes, processed to plasma, and stored at −20°C until assayed for IDS enzymatic activity.

Approximately 10–100 μL of urine was collected on days 0 (pre-treatment), 7, 14, 21, 28, 60, 74, 90, 105, and 120 and then stored at −20°C until assayed for urinary GAG levels.

Mice were euthanized on day 28 or 120 in a CO_2 fume chamber at a flow rate of 2 L/min for 3 min. The animals were perfused with 60 mL of 1× PBS (pH 7.4) in a 60-mL syringe (Becton Dickinson) with a SURFLO winged infusion set (TERUMO, Tokyo, Japan) size 23G × 3/4" with 12" tubing under hand pressure. Brain, heart, lung, liver, spleen, kidney, and quadriceps muscle were collected and dissected into 3 parts: one part for histopathologic analysis in 10% neutral-buffered formalin and the remaining parts were snap frozen and stored at −70°C until processing for assessment of IDS enzymatic activity, GAG storage, and gene modification.

At the end of study (4 months), animals were necropsied at the University of Minnesota by Seventh Wave Laboratories (Maryland Heights, MO) and tissues or tissue sections were collected and placed into 10% neutral-buffered formalin (NBF) for fixation. The following tissues were trimmed by Seventh Wave to produce histological sections: adrenal glands; aorta, brain; cecum; colon; duodenum; epididymis; esophagus; eyes; femoral-tibial joint; gallbladder; Harderian gland; heart; ileum; jejunum; kidney; larynx; lesions; liver; lungs with bronchi; lymph node (mesenteric); optic nerve; pancreas; parathyroid gland; pituitary gland; prostate gland; rectum; salivary glands; sciatic nerve; seminal vesicles; skeletal muscle (quadriceps femoris); skin; spinal cord (cervical, thoracic, and lumbar); spleen; sternum with bone marrow; stomach; testes; thymus; thyroid gland; tongue; trachea; and urinary bladder. Tissues listed above were routinely processed and embedded in paraffin blocks. The blocks were sectioned and stained with H&E. Slides were evaluated microscopically by a board-certified veterinary pathologist.

Tissue Processing

Organs were homogenized using a Bullet blender STORM bead mill homogenizer (NEXT ADVANCE) and clarified using an Eppendorf centrifuge 5424R at 13,000 rpm for 15 min at 4°C. All supernatants (tissue lysates) were transferred into new microcentrifuge tubes and stored at −20°C to −80°C until assay for IDS, GAGs, and protein content.

IDS Enzyme Assay

IDS enzyme activity was measured in tissue lysates or plasma using 4-methylumbelliferyl-α-L-iduronide-2-sulfate disodium salt (4-MU-αIdoA-2S) (Toronto Research Chemical; cat. no. M334715) as substrate in a two-step assay modified from the original protocol described by Voznyi et al.[24] In brief, tissue lysates were mixed with 1.25 mM MU-αIdoA-2S and incubated at 37°C for 1.5 hr. PiCi buffer was added to stop IDS enzyme activity. A final concentration of 1 μg/mL iduronidase (IDUA) (R&D Systems;

cat. no. 4119-GH-010) was added to start the second-step reaction and incubated overnight at 37°C. Reactions were terminated by addition of 200 µL stop buffer (0.5 M Na_2CO_3 + 0.5 M $NaHCO_3$ and 0.025% Triton X-100 [pH 10.7]) and tubes were centrifuged at 13,000 rpm for 1 min. Supernatants were transferred into a round-bottom black 96-well plate. Fluorescence was measured at excitation 365 nm and emission 450 nm using a Synergy MX plate reader and spectrophotometer (BioTek Instruments) with Gen5 plate reader program. IDS enzyme activity was expressed as nmol 4-MU per hour per mg of protein or per mL of plasma (nmol/hr/mg protein or nmol/hr/mL plasma). All reactions were run in duplicate.

GAG Assay

Tissue lysates were incubated overnight with Proteinase K, DNase1, and RNase as previously described[25] and then GAG contents in the treated samples were measured using the Blyscan Sulfated Glycosaminoglycan Assay kit (Biocolor Life Science Assays; Accurate Chemical, NY). Tissue GAG levels are expressed as µg GAG/mg protein, and urine GAG levels are expressed as µg GAG/mg creatinine (Sigma-Aldrich no. MAK080).

Mass spectrometry of brain tissue homogenates for levels of dermatan and heparan sulfate was performed at Pacific BioLabs (Hercules, CA). Briefly, tissues were homogenized in 200 mM ammonium acetate, 20 mM calcium acetate, 4 mM DTT (pH 7.0). Protein concentrations were determined by BCA Protein Assay Kit (Thermo Fisher Scientific), and samples were normalized to 1 mg/mL. Heparan sulfate samples were digested with heparinase I and III, yielding two major disaccharides (Δ-UA-GlcNAc [IV-A] and Δ-UA-GlcNS [IV-S]). Dermatan sulfate samples were digested with chondroitinase B, yielding 3 major disaccharides (ΔUA-GalNAc [4S] [Δdi-4S], ΔUA-GalNAc [6S] [Δdi-6S], and ΔUA-GalNAc [4S, 6S] [Δdi-4S,6S]). After digestion, an internal standard (ΔUA2S-GlcNCOEt6S) was spiked in, large molecules were removed by centrifuging through a 10,000 NMWL spin filter, and samples were subjected to reversed-phase high-performance liquid chromatography (HPLC). Heparan sulfate and dermatan sulfate disaccharides were separated on a Thermo Hypercarb column (5 µm; 50 × 2.1 mm; P/N 35005-052130) with a 25 mM ammonium acetate, 6 mM tributylamine (pH 7) solvent system using a gradient curve from 0% to 100% solvent B (80% acetonitrile) at a flow rate of 0.4 mL/min. Analytes and internal standards were detected via ESI-MS/MS (Applied Biosystems API 4000 QTRAP) using a specific multiple-reaction-monitoring method in negative mode (458→300 for Δdi-4S; 458→282 for Δdi-6S; 538→458 for Δdi-4S,6S; 378→175 for IV-A; 416→138 for IV-S; and 552→472 for international standard [IS]). The peaks of each analyte and IS were integrated in their respective mass spectrometry (MS) chromatogram, and the ratios of the analyte/IS peak areas were used for quantitation. Concentrations of respective disaccharides in unknown samples were interpolated from a calibration curve of standards at known concentration and are reported in µg/mL, with a lower limit of quantitation (LLOQ) of 0.005 µg/mL for each disaccharide. Disaccharide concentrations were summed for each sample and plotted relative to homogenate input.

Behavioral Testing

The Barnes maze is a circular platform measuring approximately 4 feet in diameter and is elevated approximately 4 feet from the floor with 40 holes spaced equally around the perimeter. All of the holes are blocked except one to allow the mouse to escape the platform. Visual cues were attached to each of the 4 walls for the mouse to use as spatial navigators. In the final week of the study (approximately 4 months post-dosing), mice were placed in the middle of the platform with an opaque funnel covering the animal. The cover was lifted, releasing the mouse and exposing it to bright light. Mice were given 3 min to escape the platform. Mice were subjected to 4 trials per day for a total of 6 days.

IDS Western Blot

Approximately 50 mg of frozen liver tissue was homogenized in radioimmunoprecipitation assay (RIPA) buffer using Lysis Matrix D tubes on a FastPrep-24 instrument (MP Biomedicals). Protein concentration was determined using the Pierce bicinchoninic acid (BCA) Protein Assay Kit (Thermo Fisher Scientific) prior to IDS detection by western blot using a LI-COR Odyssey scanner (LI-COR Biotechnology, Lincoln, NE). Antibodies used were IDS (AF2449; R&D Systems) and glyceraldehyde 3-phosphate dehydrogenase (GAPDH) (A00191; GenScript; conjugated to DyLight 800 using the Lightning-Link conjugation kit [Novus Biologicals]).

Indel Detection by Next-Generation Sequencing

Genomic DNA was isolated from the liver of each mouse, and the ZFN target site was amplified by PCR. The MiSeq system (Illumina) was used for paired-end deep sequencing to determine the level of modification. SeqPrep software (https://github.com/jstjohn/SeqPrep) was used to align and merge paired sequences. The Needleman-Wunsch algorithm was used to compare individual sequences with the wild-type sequence[26] and to map indels. ZFN activity is reported as "% indels," the fraction of sequenced amplicons that differ from wild-type due to insertions or deletions.

Statistical Analysis

All values are presented as mean ± SEM or mean ± SD. GraphPad Prism software was used to perform statistical analyses. Differences among treated groups for tissue IDS activity and GAG levels were evaluated using the nonparametric Kruskal-Wallis test. For plasma IDS activity and Barnes maze, data from all groups were compared to wild-type by two-way repeated-measures ANOVA followed by Dunnett's multiple comparisons test.

SUPPLEMENTAL INFORMATION

Supplemental Information includes Supplemental Materials and Methods, four figures, and one table and can be found with this article online at https://doi.org/10.1016/j.ymthe.2018.03.002.

AUTHOR CONTRIBUTIONS

K.L., R.C.D., K.E.M., M.C.H., C.B.W., T.W., and R.S.M. designed the experiments. K.L., R.C.D., K.M.P.-P., M.R., S.S., H.O.N., T.N., S.J.S.M., L.O., S.T., T.W., and R.R. generated reagents, performed

the experiments, and analyzed data. K.L., R.C.D., K.E.M., M.C.H., T.W., and R.S.M. wrote and revised the manuscript.

CONFLICTS OF INTEREST

R.C.D., M.R., S.S., H.O.N., S.J.S.M., S.T., R.R., K.E.M., M.C.H., and T.W. are employees of Sangamo Therapeutics. C.B.W. is a paid consultant of Sangamo Therapeutics. The remaining authors declare no competing interests.

ACKNOWLEDGMENTS

We are grateful to Dr. Joseph Muenzer for providing the MPS II mouse strain. The authors would like to thank Carolyn Gaspar, Annemarie Ledeboer, Melanie Butler, Marshall Huston, and Amy Manning-Bog for assistance in necropsy and figure preparation and also Seventh Wave Laboratories (Maryland Heights, MO) for performing necropsy and histopathology evaluation (Mark Martinez, DVM, DACVP) and Pacific BioLabs (Hercules, CA) for performing mass spectrometry analysis of dermatan and heparan sulfate levels (Rick Staub and Vy Tran). This work was supported by Sangamo Therapeutics. The materials described herein will be provided upon request after execution of a material transfer agreement with the University of Minnesota and/or Sangamo Therapeutics, as appropriate.

REFERENCES

1. Nathwani, A.C., Reiss, U.M., Tuddenham, E.G.D., Rosales, C., Chowdary, P., McIntosh, J., Della Peruta, M., Lheriteau, E., Patel, N., Raj, D., et al. (2014). Long-term safety and efficacy of factor IX gene therapy in hemophilia B. N. Engl. J. Med. *371*, 1994–2004.
2. Bennett, J., Ashtari, M., Wellman, J., Marshall, K.A., Cyckowski, L.L., Chung, D.C., McCague, S., Pierce, E.A., Chen, Y., Bennicelli, J.L., et al. (2012). AAV2 gene therapy readministration in three adults with congenital blindness. Sci. Transl. Med. *4*, 120ra15.
3. Sharma, R., Anguela, X.M., Doyon, Y., Wechsler, T., DeKelver, R.C., Sproul, S., Paschon, D.E., Miller, J.C., Davidson, R.J., Shivak, D., et al. (2015). In vivo genome editing of the albumin locus as a platform for protein replacement therapy. Blood *126*, 1777–1784.
4. Li, H., Haurigot, V., Doyon, Y., Li, T., Wong, S.Y., Bhagwat, A.S., Malani, N., Anguela, X.M., Sharma, R., Ivanciu, L., et al. (2011). In vivo genome editing restores haemostasis in a mouse model of haemophilia. Nature *475*, 217–221.
5. Lombardo, A., Genovese, P., Beausejour, C.M., Colleoni, S., Lee, Y.-L., Kim, K.A., Ando, D., Urnov, F.D., Galli, C., Gregory, P.D., et al. (2007). Gene editing in human stem cells using zinc finger nucleases and integrase-defective lentiviral vector delivery. Nat. Biotechnol. *25*, 1298–1306.
6. Genovese, P., Schiroli, G., Escobar, G., Tomaso, T.D., Firrito, C., Calabria, A., Moi, D., Mazzieri, R., Bonini, C., Holmes, M.C., et al. (2014). Targeted genome editing in human repopulating haematopoietic stem cells. Nature *510*, 235–240.
7. Anguela, X.M., Sharma, R., Doyon, Y., Miller, J.C., Li, H., Haurigot, V., Rohde, M.E., Wong, S.Y., Davidson, R.J., Zhou, S., et al. (2013). Robust ZFN-mediated genome editing in adult hemophilic mice. Blood *122*, 3283–3287.
8. Muenzer, J., Lamsa, J.C., Garcia, A., Dacosta, J., Garcia, J., and Treco, D.A. (2002). Enzyme replacement therapy in mucopolysaccharidosis type II (Hunter syndrome): a preliminary report. Acta Paediatr. Suppl. *91*, 98–99.
9. Friso, A., Tomanin, R., Alba, S., Gasparotto, N., Puicher, E.P., Fusco, M., Hortelano, G., Muenzer, J., Marin, O., Zacchello, F., and Scarpa, M. (2005). Reduction of GAG storage in MPS II mouse model following implantation of encapsulated recombinant myoblasts. J. Gene Med. *7*, 1482–1491.
10. Cardone, M., Polito, V.A., Pepe, S., Mann, L., D'Azzo, A., Auricchio, A., Ballabio, A., and Cosma, M.P. (2006). Correction of Hunter syndrome in the MPSII mouse model by AAV2/8-mediated gene delivery. Hum. Mol. Genet. *15*, 1225–1236.
11. Garcia, A.R., Pan, J., Lamsa, J.C., and Muenzer, J. (2007). The characterization of a murine model of mucopolysaccharidosis II (Hunter syndrome). J. Inherit. Metab. Dis. *30*, 924–934.
12. Bielicki, J., Hopwood, J.J., Wilson, P.J., and Anson, D.S. (1993). Recombinant human iduronate-2-sulphatase: correction of mucopolysaccharidosis-type II fibroblasts and characterization of the purified enzyme. Biochem. J. *289*, 241–246.
13. Kwok, J.C.F., Warren, P., and Fawcett, J.W. (2012). Chondroitin sulfate: a key molecule in the brain matrix. Int. J. Biochem. Cell Biol. *44*, 582–586.
14. Ohashi, T., Watabe, K., Uehara, K., Sly, W.S., Vogler, C., and Eto, Y. (1997). Adenovirus-mediated gene transfer and expression of human beta-glucuronidase gene in the liver, spleen, and central nervous system in mucopolysaccharidosis type VII mice. Proc. Natl. Acad. Sci. USA *94*, 1287–1292.
15. Nathwani, A.C., Gray, J.T., McIntosh, J., Ng, C.Y.C., Zhou, J., Spence, Y., Cochrane, M., Gray, E., Tuddenham, E.G., and Davidoff, A.M. (2007). Safe and efficient transduction of the liver after peripheral vein infusion of self-complementary AAV vector results in stable therapeutic expression of human FIX in nonhuman primates. Blood *109*, 1414–1421.
16. Stocker, J.T., Dehner, L.P., and Husain, A.N. (2012). Stocker and Dehner's Pediatric Pathology (Philadelphia, PA: Lippincott Williams & Wilkins).
17. Barzel, A., Paulk, N.K., Shi, Y., Huang, Y., Chu, K., Zhang, F., Valdmanis, P.N., Spector, L.P., Porteus, M.H., Gaensler, K.M., and Kay, M.A. (2015). Promoterless gene targeting without nucleases ameliorates haemophilia B in mice. Nature *517*, 360–364.
18. Ou, L., Herzog, T., Koniar, B.L., Gunther, R., and Whitley, C.B. (2014). High-dose enzyme replacement therapy in murine Hurler syndrome. Mol. Genet. Metab. *111*, 116–122.
19. Blanz, J., Stroobants, S., Lüllmann-Rauch, R., Morelle, W., Lüdemann, M., D'Hooge, R., Reuterwall, H., Michalski, J.C., Fogh, J., Andersson, C., and Saftig, P. (2008). Reversal of peripheral and central neural storage and ataxia after recombinant enzyme replacement therapy in alpha-mannosidosis mice. Hum. Mol. Genet. *17*, 3437–3445.
20. Matzner, U., Lüllmann-Rauch, R., Stroobants, S., Andersson, C., Weigelt, C., Eistrup, C., Fogh, J., D'Hooge, R., and Gieselmann, V. (2009). Enzyme replacement improves ataxic gait and central nervous system histopathology in a mouse model of metachromatic leukodystrophy. Mol. Ther. *17*, 600–606.
21. Polito, V.A., Abbondante, S., Polishchuk, R.S., Nusco, E., Salvia, R., and Cosma, M.P. (2010). Correction of CNS defects in the MPSII mouse model via systemic enzyme replacement therapy. Hum. Mol. Genet. *19*, 4871–4885.
22. Rozaklis, T., Beard, H., Hassiotis, S., Garcia, A.R., Tonini, M., Luck, A., Pan, J., Lamsa, J.C., Hopwood, J.J., and Hemsley, K.M. (2011). Impact of high-dose, chemically modified sulfamidase on pathology in a murine model of MPS IIIA. Exp. Neurol. *230*, 123–130.
23. Doyon, Y., Vo, T.D., Mendel, M.C., Greenberg, S.G., Wang, J., Xia, D.F., Miller, J.C., Urnov, F.D., Gregory, P.D., and Holmes, M.C. (2011). Enhancing zinc-finger-nuclease activity with improved obligate heterodimeric architectures. Nat. Methods *8*, 74–79.
24. Voznyi, Y.V., Keulemans, J.L., and van Diggelen, O.P. (2001). A fluorimetric enzyme assay for the diagnosis of MPS II (Hunter disease). J. Inherit. Metab. Dis. *24*, 675–680.
25. Wolf, D.A., Lenander, A.W., Nan, Z., Belur, L.R., Whitley, C.B., Gupta, P., Low, W.C., and McIvor, R.S. (2011). Direct gene transfer to the CNS prevents emergence of neurologic disease in a murine model of mucopolysaccharidosis type I. Neurobiol. Dis. *43*, 123–133.
26. Needleman, S.B., and Wunsch, C.D. (1970). A general method applicable to the search for similarities in the amino acid sequence of two proteins. J. Mol. Biol. *48*, 443–453.